Validation and Comparison of Two AOMA Approaches for the Ambient Vibration Testing of Long Suspension Bridges Under Strong Wind Loads

Validation and comparison of two AOMA approaches for the Ambient Vibration Testing of long suspension bridges under strong wind loads

Marco Civera[1[0000-0003-0414-7440]], Marco Martino Rosso[1 [0000-0002-9098-4132]], Giuseppe Carlo Marano[1[0000-0001-8472-2956]], and Bernardino Chiaia[1[0000-0002-5469-2271]]

[1] Department of Structural, Geotechnical and Building Engineering, Politecnico di Torino, Corso Duca degli Abruzzi 24, Turin 10129, Italy
marco.civera@polito.it

Abstract. Several Automated Operational Modal Analysis (AOMA) approaches have been developed in the last few years. Among them, two recent data-driven, Machine Learning (ML) techniques have been selected for comparison. The first one uses a combination of two clustering algorithms (k-means with k=2 and density-based clustering). The second one uses kernel density estimation (KDE) for the interpretation of the stabilization diagram and therefore the selection of stable pole alignments. Both algorithms have been previously validated on applications for Civil Engineering purposes. In this work, the two approaches are validated and directly compared for the first time for the Structural Health Monitoring of long suspension bridges. A compelling experimental case study is considered: the Hardanger Bridge dataset. This infrastructure crosses the Hardangerfjord in Norway, with a total length of 1380 m (1310 m in the central span alone, making it one of the longest suspension bridge spans in the world). The experimental data investigated here represent an interesting stress test for the capabilities of the two methods, since the bridge has several closely-spaced, very low frequency (<1 Hz) modes, due to its slenderness and flexibility. Not only that, the bridge is inserted in a harsh environment, subject to Atlantic storms and a complicated wind field around due to the local topography with steep mountains and wide fjords. Hence, this work also briefly assesses the potential applications of the proposed code for handling changing ambient conditions.

Keywords: Operational Modal Analysis, Ambient Vibration Test, Bridge Monitoring, Suspension Bridge, Operational and Environmental Effects, Wind Loads.

1 Introduction

Structural Health Monitoring (SHM) is a critical aspect of Bridge Engineering, as it ensures the safety and longevity of these vital infrastructures. This is particularly im-

portant for less common typologies such as slender, long-span, and relatively lightweight steel-made suspension bridges.

Unlike other more conventional bridges, which often have bulkier designs and shorter spans, suspension bridges feature streamlined configurations with expansive lengths, often surpassing a kilometre. These strong dissimilarities in the stiffness-to-weight ratio pose unique challenges for dynamic monitoring, demanding specialized attention. To begin with, even in still air and default ambient conditions, their dynamic behaviour is markedly different, with much lower natural frequencies. Furthermore, this inherent slenderness introduces complexities in their behaviour under varying operational and environmental conditions, including wind, traffic, and thermal loads. Consequently, monitoring systems for these bridges must adapt to account for their sensitivity to dynamic forces, ensuring precision in detecting potential structural changes. A recent and interesting review of such applications can be found in [1]. Therefore, the application of Ambient Vibration Testing (AVT), Operational Modal Analysis (OMA), and Automated Operational Modal Analysis (AOMA) [2] is particularly challenging for these infrastructures. Many techniques that can be considered viable for reinforced concrete (RC) bridges, with their relatively high and well-spaced natural frequencies, scarcely affected by wind and other conditions, could not withstand these increased difficulties.

Hence, two recent AOMA algorithms, proposed by some of the Authors independently in [3] and [4], are here compared and benchmarked on the Hardanger Bridge Experimental Dataset [5]. This short study includes the identified modal parameters for three different ambient conditions (still air, average windy day, and storm). The results prove that both methodologies are viable for such competing applications; in particular, both methods are able to correctly identify the natural frequencies of the benchmark structure under investigation.

2 The two methodologies

Hereinafter, the focal aspects of the two algorithms tested in this comparative analysis are briefly explained. Importantly, the first one (the DBSCAN-based approach) was developed in a Matlab environment. The second, instead, is known as intelligent AOMA (i-AOMA) and was developed as a Python script.

2.1 DBSCAN-based AOMA

The first approach, whose flowchart is depicted in Figure 1, uses density-based and k-means clustering. A detailed explanation of the several technical aspects can be found in [3]. A previous application for the Structural Health Monitoring of an R.C. road bridge can be found in [6]. Only the main points are recalled here for completeness.

The code was implemented as a Matlab function and tested on version R2022a. The fully automatic approach interprets the stabilisation diagram following these five sequential steps:

1) Identification of candidate poles by the covariance-driven Stochastic Subspace Identification (SSI-COV) method [7], for a range of model orders, n, included between an arbitrary minimum, n_{min}, and maximum, n_{max}.
2) Preliminary sifting based on Hard Validation Criteria (HVC).
3) Subsequent distinction (and further sifting) of poles into stable and unstable sets by Soft Validation Criteria (SVC) [3-6].
4) Clustering of the remaining poles; third (and final) sifting, discerning certainly mathematical (CM) and probably physical (PP) clusters, then discarding the former ones.
5) Final estimation of the cluster-wide modal parameters.

The difference between the DBSCAN-based approach and the conventional hierarchical-clustering methodology as reported e.g. [8] and [9] resides in the use, after HVC and SVC, of the clustering algorithm proposed by [10]. Without going into too much detail, the method requires a certain distance epsilon (ε) and a minimum number of data points required (*MinPts*), directly estimated by the data [3].

At this point, having defined all the clusters of the twice-sifted poles, the clusters are evaluated based on their population. Low-populated clusters are labelled as CM and discarded; only highly populated ones are passed on to the very last step, where the modal parameters of all poles inside the same cluster are averaged and returned as the final result. However, this last part of the algorithm (based on k-means clustering, with k=2 to binary classify the clusters as CM or PP), is again identical to [9] and other previous works from other authors.

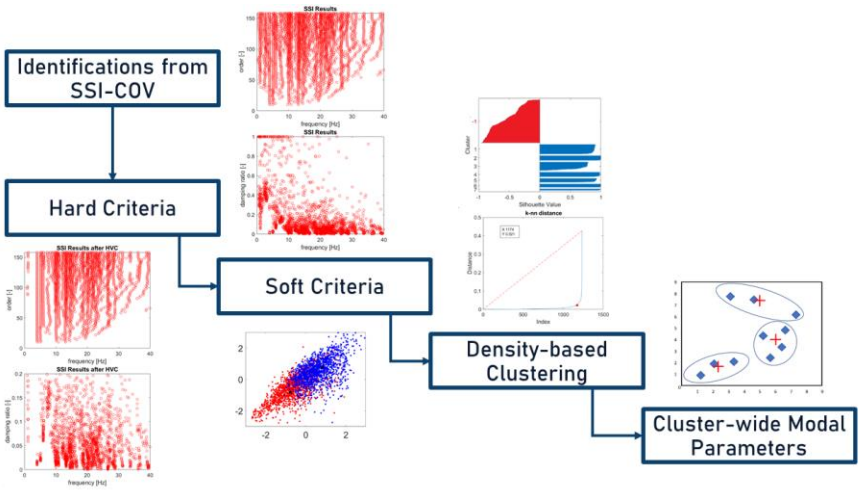

Fig. 1. Flowchart of DBSCAN-based AOMA method. Based on the example reported in [6]

2.2 Intelligent-based AOMA

The second approach, whose schematic flowchart is depicted in Figure 2, is fully described in [4]. A version of the code, implemented in Python, is freely downloadable at https://github.com/marco-rosso-m/i-AOMA.

With respect to the previous algorithm, the main differences lie in the adoption of a Quasi-Monte-Carlo-based strategy and multiple runs of the already-mentioned covariance-driven Stochastic Subspace Identification (SSI-COV). The method is organised in a two-step procedure. The first phase is demanded to run a predefined number of simulations to collect the stabilization diagram results. This ensures a random selection of the SSI-COV governing parameters, viz. the Hankel block rows number, the maximum order, the time window slicing length of the entire recording, and the target time where centring the time window slicing. After collecting several stabilization diagrams, the HVC and SVC are used to retain only the stable poles. The stabilization diagrams are all overlapped and post-processed with a kernel density estimation (KDE) algorithm [10] to identify the stable pole alignments, thus identifying the modes of interest. Another key difference with the previously described method is the adoption of a KDE algorithm rather than an ML clustering approach. An information content metric (IC_k) is computed for every simulation k to express the quality of the results for every set of governing parameters in providing several stable retained poles $N_{stp,k}$ concerning all the stable and unstable poles computed $N_{totp,k}$.

Phase 2 of the algorithm starts with training a random forest (RF) algorithm based on the sampled sets of governing parameters and their relative IC_k. In this way, the RF can intelligently drive the subsequent sampling of governing parameters saving computational resources by discarding those sets that are predicted to provide very low IC_k. The acceptable shifting convergence band rule (ASCBR) [11] acts as a stopping criterion, i.e. when the total sample variance of the considered modes exhibits a variation limited within the 2% for the last 50 simulations. After reaching the convergence, the overlapped stabilization diagrams are again post-processed with the KDE to select the stable pole alignments. The modal parameters and their relative uncertainties can be eventually computed.

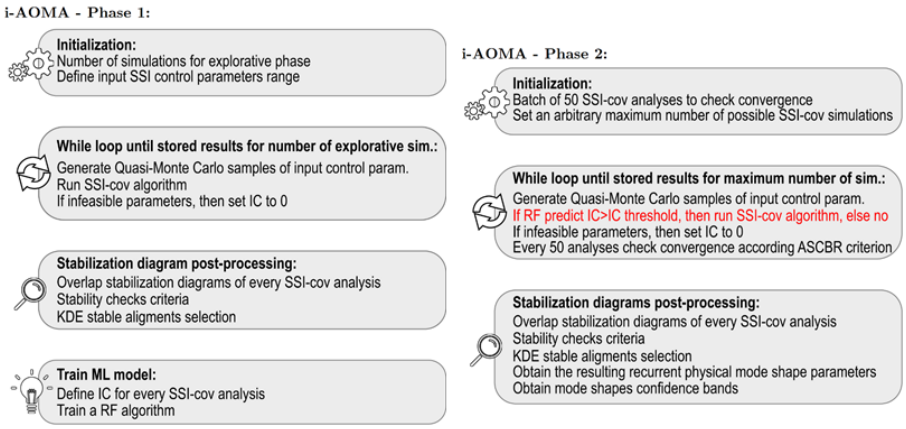

Fig. 2. Schematic flowchart of intelligent AOMA method, evidencing main steps of Phase 1 and Phase 2 of the method.

3 Description of the Hardanger Bridge Experimental Benchmark

The complete and detailed description of the case study and its permanent monitoring system can be found in [5]. To keep this discussion self-sustained, only the key aspects are recalled here.

3.1 The structure and its permanently installed monitoring system.

The Hardanger Bridge (portrayed in Figure 3) is Norway's longest suspension bridge, spanning 1,308 meters with short spans on both sides. It is also enclosed between two tunnels. Despite the slender design of the steel box deck, it is capable of carrying two traffic lanes and a bike lane. 200-meter-high pylons support the girder, held by two main cables and 130 hangers, the length of which ranges from 2 to 128 meters. The bridge was initially equipped with 20 accelerometers and nine anemometers. As will be discussed in the next Sections, only a subset of them was continuously used throughout the years. The system had eight anemometers placed 8 meters from the girder to avoid disrupting wind flow. However, as of September 2018, wind speed monitoring ceased at the tower tops following the removal of one sensor from the Vallavik tower. For all these reasons, this case study represents a very compelling experimental benchmark, both for structural and environmental reasons. On the one hand, its fundamental vibrational modes are all clustered at very low frequencies (below 1 Hz) and very closely spaced. On the other hand, its specific building material, structural configuration, and location make it very susceptible to environmental effects (wind speed and pattern, specifically). All these aspects provide an interesting stress test for the two proposed procedures.

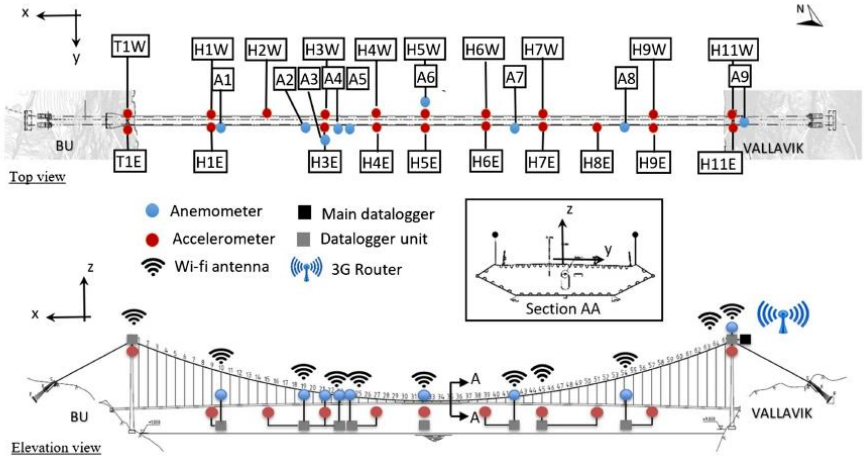

Fig. 3. Plan and side view of the Hardanger Bridge with its instrumentation. Retrieved from [5]

3.2 Target values

To produce results directly comparable to the ones of [13], the following precautions have been adopted:

1. The original data, sampled at f_s = 200 Hz, have been used.
2. These have been decimated by a factor of 20, thus focusing only on the 0-10 Hz range;
3. Frequencies higher than f_{up} = 10 Hz have been discarded;
4. The range of model orders has been set from n_{min} = 20 to n_{max} = 200.

These steps replicate the procedure of [13], for which the authors of the original dataset obtained the target values reported in Table 1.

Table 1. Experimentally identified natural frequencies and damping ratios.

mode ID number	description	source	$f_{n,target}$ [Hz]	$\xi_{n,target}$ [%]
1	symmetric horizontal (1st lagging)	experimental [13]	0.05	1.07
2	symmetric vertical (1st flapping)	experimental [13]	0.14	2.27
3	symmetric horizontal (2nd lagging)	numerical [14]	0.17	n.a.
4	symmetric vertical (2nd flapping)	experimental [13]	0.21	2.75
5	symmetric torsional (1st torsional)	experimental [13]	0.37	0.90

As mentioned in Table 1, mode f_3 is not reported in [13] but rather estimated from a series of numerical simulations and experimental evidence collected in [14]. This is included as it was confirmed by the results of this study.

It is important to state that the values retrieved from [13] refer specifically to the results obtained by the application of the MACEC software developed at the University of Leuven [15], specifically using the SSI-COV algorithm (as both SSI-COV and SSI-DATA were provided but this latter variant is generally deemed as less accurate [2]).

3.3 Selected signals and output channels

The results retrieved from [13] and reported in Table 1 specifically refer to a condition of sustained wind (16 m/s). Indeed, in [14], it is also explicitly stated how the measurement system is set to be triggered when a wind speed of at least 15 m/s is exceeded at any of the anemometers. Without anticipating too much from the Results section, this is reasonable as relatively higher wind speeds were found to excite lateral modes, making them much easier to identify. Thus, to enforce fair comparability between this and other works from the authors of the original dataset, a similar wind condition was considered, with an average speed of 14 m/s. To better investigate the

well-documented effects of wind speed on the modal parameters of the structure [5,13,14], two other conditions are included as well: almost still air (very low wind speed, below 2 m/s) and storm conditions (taken from the Tina storm event of October 2015). These are detailed here below:

1. Case 1: 2015-11-14 at 03:52:21 (wind speed: 1.86 ± 0.38 m/s);
2. Case 2: 2015-11-12 at 23:54:31 (wind speed: 14.02 ± 2.28 m/s), shown in Figure 4;
3. Case 3: 2015-01-10 at 16:22:08 (wind speed: 24.26 ± 4.27 m/s).

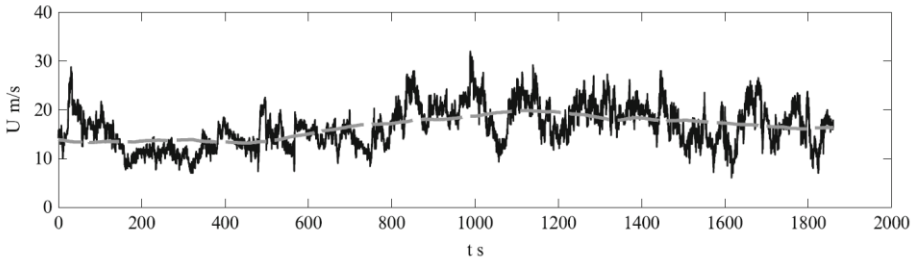

Fig. 4. Graph of wind speed recording at the mid-span anemometer (A6) corresponding to the target values (retrieved from [13]) in medium wind speed situation, i.e. case 2.

Unfortunately, out of the 20 triaxial accelerometers described in [5] and recalled in the previous sections, only 12 (namely, H2W, H4E, H4W, H5E, H5W, H6E, H6W, H7E, H7W, H8E, H10E, and H10W) were available for the last case (Tina Storm). To uniform the results, only this subset of sensors was used for the first two cases as well, for a total of 36 output channels available. For all sensors, the channel orientations followed the global reference frame, with the x-axis oriented longitudinally along the bridge (positive direction from Vallavik to Bu), the y-axis transversally to the bridge (positive towards East), and the z-axis following the vertical direction (positive upwards).

4 Results

For all cases, the results reported here are defined according to precautions described previously in Sect. 3.3 For the case with average wind speed (Case 2), the results for the DBSCAN-based, Matlab-developed AOMA code are reported in the third and fourth columns of Table 2, with the values rounded up to the second decimal digit. The percentage error is computed as follows:

$$\Delta = 100 \cdot (X_{n,ID} - X_{n,target}) / X_{n,target} \quad (1)$$

Where X indicates a generic parameter (here, natural frequencies or damping ratios).

Table 2. Results for the DBSCAN-based, Matlab-developed AOMA and the Python-developed i-AOMA codes, rounded up to the second decimal place.

mode ID number	description	DBSCAN AOMA		i-AOMA	
		$f_{n,ID}$ [Hz]	$\xi_{n,ID}$ [%]	$f_{n,ID}$ [Hz]	$\xi_{n,ID}$ [%]
1	symmetric horizontal (1st lagging)	0.05 (0%)	0.96 (−10.28%)	0.05 (0%)	2.10 (+96.26%)
2	symmetric vertical (1st flapping)	0.14 (0%)	2.28 (+0.44%)	0.14 (0%)	2.22 (−2.20%)
3	symmetric horizontal (2nd lagging)	0.19 (+11.74%)	0.86 (n.a)	0.19 (+8.13%)	0.72 (n.a.)
4	symmetric vertical (2nd flapping)	0.21 (0%)	1.12 (−59.27%)	0.21 (−1.42%)	1.41 (−48.73%)
5	symmetric torsional (1st torsional)	0.37 (0%)	0.99 (+10.00%)	0.37 (−0.81%)	1.01 (+12.12%)

As can be seen, the results are very consistent frequency-wise, also considering that the vibration time series, while expected to be similar due to similar wind excitation, is not exactly the same. The main divergence can be found in the damping ratios of the higher modes. However, damping ratios are well-known to be difficult to estimate with high precision and susceptible to higher variability from one recording to the other [16]. Moreover, these are also very sensible to even slight changes in this environmental parameter [13,14]. Thus, even the slight difference from the target benchmark (14 m/s rather than circa 16 m/s) can explain these inconsistencies.

The fifth and sixth columns of the same Table mirror the results for the second algorithm, demonstrating that the i-AOMA results are frequency-wise consistent with the reference values as well. Nonetheless, even in this case, the greater scatter is exhibited by the particularly high damping ratio, especially for the first mode. This confirms that the uncertainties related to the damping ratio are still high also in this second independent procedure. Similar results were obtained for the other two cases (with lower and higher wind speeds); these are not reported due to space limitations.

By comparing the two methodologies, one can observe that both procedures are able to identify closely spaced modes in terms of natural frequencies. The damping ratios still exhibit a quite large difference between the two methodologies, and even among the different wind cases. For instance, in i-AOMA, the overall lowest damping ratios are exhibited with the lowest wind speed conditions, thus evidencing that a lower damping effect is activated by the structures without enough wind excitation. A further direct comparison between the two techniques can be made in terms of the Modal Assurance Criterion (MAC) values between the estimated mode shapes. DBSCAN-based method and i-AOMA technique provided a MAC of 0.81 for the mode at 0.05 Hz and above 0.98 for the other modes, except for the mode at 0.19 Hz. In this regard, the shape of this third mode evidenced that the DBSCAN-based method provided a pure horizontal mode, in accordance with the reference. In contrast, the i-AOMA provided a mixed horizontal and vertical mode, thus possibly explaining

why the MAC exhibited a correlation of 0.55 with the mode at 0.14 Hz and 0.69 with the mode at 0.21 Hz.

5 Discussion and Conclusions

In this short contribution, two state-of-the-art AOMA algorithms, developed independently by some of the Authors, have been compared and benchmarked on a very compelling case study for bridge monitoring applications. The DBSCAN-based algorithm, first introduced for Aerospace applications and already validated for R.C. bridges, has been further validated for the much more difficult task of the dynamic identification of long-span suspension bridges. The i-AOMA approach, previously tested for slender high-rise buildings, similarly demonstrated its successful performance in properly identifying closely spaced modes of the current suspension Hardanger Bridge case study. Both methodologies still evidenced some differences in terms of damping ratio, but this is well-known to be one of the most debated parts in the existing literature. Future studies will provide more insights and investigations into a possible integration of strong points of both AOMA methodologies to improve the current algorithms with always smarter and more reliable implementations.

Acknowledgements

This work is part of the research activity developed by the authors Marco Civera and Bernardino Chiaia within the framework of the ``PNRR'': SPOKE 7 ``CCAM, Connected Networks and Smart Infrastructure'' - WP4.

Giuseppe Carlo Marano and Marco Martino Rosso acknowledge the support from PNRR MUR project PE0000013-FAIR (National Recovery and Resilience Plan -- NRRP, Mission 4, Component 2, Investment 1.3, NextGenerationEU -- D.D. 341 15/3/2022 and D.D. 1555 11/10/2022, PE0000013).

References

1. Dederichs, A.C., Øiseth, O.: Experimental comparison of automatic operational modal analysis algorithms for application to long-span road bridges. Mechanical Systems and Signal Processing 199, 110485 (2023)
2. Rainieri, C., Fabbrocino, G.: Operational modal analysis of civil engineering structures. Springer, New York 142, 143 (2014).
3. Sibille, L., Civera, M., Zanotti Fragonara, L., Ceravolo, R.: Automated operational modal analysis of a helicopter blade with a density-based cluster algorithm. AIAA Journal 61(3), 1411–1427 (2023)
4. Rosso, M.M., Aloisio, A., Parol, J., Marano, G.C., Quaranta, G.: Intelligent automatic operational modal analysis. Mechanical Systems and Signal Processing 201, 110669 (2023)
5. Fenerci, A., Andreas Kvåle, K., Wiig Petersen, Ø., Rønnquist, A., Øiseth, O.: Data set from long-term wind and acceleration monitoring of the hardanger bridge. Journal of Structural Engineering 147(5), 04721003 (2021)

6. Civera, M., Sibille, L., Fragonara, L.Z., Ceravolo, R.: A dbscan-based automated operational modal analysis algorithm for bridge monitoring. Measurement 208, 112451 (2023)
7. Van Overschee, P., De Moor, B.: Subspace identification for linear systems: Theory—Implementation—Applications. Springer Science & Business Media (2012)
8. Reynders, E., Houbrechts, J., De Roeck, G.: Fully automated (operational) modal analysis. Mechanical systems and signal processing 29, 228–250 (2012)
9. Mugnaini, V., Fragonara, L.Z., Civera, M.: A machine learning approach for automatic operational modal analysis. Mechanical Systems and Signal Processing 170, 108813 (2022)
10. Ester, M., Kriegel, H.P., Sander, J., Xu, X., et al.: A density-based algorithm for discovering clusters in large spatial databases with noise. In: kdd. vol. 96, pp. 226–231 (1996)
11. Gramacki, A.: Nonparametric kernel density estimation and its computational aspects, vol. 37. Springer (2018)
12. Ata, M.Y.: A convergence criterion for the monte carlo estimates. Simulation Modelling Practice and Theory 15(3), 237–246 (2007)
13. Øiseth, O., Rönnquist, A., Kvåle, K.A., Sigbjörnsson, R.: Monitoring wind velocities and dynamic response of the hardanger bridge. In: Dynamics of Civil Structures, Volume 2: Proceedings of the 33rd IMAC, A Conference and Exposition on Structural Dynamics, 2015. pp. 117–125. Springer (2015)
14. Fenerci, A., Øiseth, O.: The hardanger bridge monitoring project: Long-term monitoring results and implications on bridge design. Procedia engineering 199, 3115–3120 (2017)
15. Peeters, B., De Roeck, G.: Reference-based stochastic subspace identification for output-only modal analysis. Mechanical systems and signal processing 13(6), 855–878 (1999)
16. Colmenares, D., Costa, G., Civera, M., Surace, C., Karoumi, R.: Quantification of the human–structure interaction effect through full-scale dynamic testing: The folke bernadotte bridge. In: Structures. vol. 55, pp. 2249–2265. Elsevier (2023).